

Unravelling the chemical inhomogeneity of PNe with VLT FLAMES integral-field unit spectroscopy

Y. G. Tsamis¹, J. R. Walsh², D. Péquignot³, M. J. Barlow¹,
X.-W. Liu⁴, and I. J. Danziger⁵

¹Dept. of Physics & Astronomy, University College London, London WC1E 6BT, U. K.

²European Southern Observatory, D-85748 Garching, Germany

³LUTH, Observatoire de Meudon-Paris, F-92195 Meudon, France

⁴Dept. of Astronomy, Peking University, Beijing, China

⁵Osservatorio di Trieste, I-34131 Trieste, Italy

Abstract. Recent weak emission-line long-slit surveys and modelling studies of PNe have convincingly argued in favour of the existence of an unknown component in the planetary nebula plasma consisting of cold, hydrogen-deficient gas, as an explanation for the long-standing recombination-line versus forbidden-line temperature and abundance discrepancy problems. Here we describe the rationale and initial results from a detailed spectroscopic study of three Galactic PNe undertaken with the VLT FLAMES integral-field unit spectrograph, which advances our knowledge about the small-scale physical properties, chemical abundances and velocity structure of these objects across a two-dimensional field of view, and opens up for exploration an uncharted territory in the study and modelling of PNe and photoionized nebulae in general.

Keywords. planetary nebulae: individual (NGC 5882, NGC 6153, NGC 7009); ISM: abundances; line: profiles

1. Introduction

In recent years, extensive weak emission-line surveys of PNe have all focused on the optical recombination-line (ORL) spectra of carbon, nitrogen, oxygen and neon ions, and the comparison between abundances derived from ORLs versus those from the bright collisionally excited lines (CELs) of these objects (Tsamis et al. 2003b, 2004; Liu et al. 2004; Wesson et al. 2005). These studies show that for the majority of PNe abundances of the above elements, relative to hydrogen, from ORLs are a factor of 2–3 higher than the corresponding CEL values. For about 5–10% of PNe however, the abundance discrepancy factors (ADF) are in the range of 4–80. Important correlations have been demonstrated such as those between the ADFs for a range of ions and the difference between the [O III] and Balmer jump temperatures, or between the ADF and the PN radius and intrinsic brightness, whereby larger/fainter (and arguably older) PNe display higher ADFs than more compact, young objects. All the above surveys, however, were based on data secured with spectrographs using long-slits (e.g. ESO 1.52-m Boller & Chivens, NTT 3.5-m EMMI) operated either at fixed nebular positions or in some cases scanned across the nebular surface, thus yielding average spectra of a given target with the unavoidable loss of spatial information in the direction perpendicular to the slit. A handful of studies charted the ORL/CEL abundances, the ADF behaviour and other nebular properties along the useful slit length for a few PNe (e.g. NGC 6153, Liu et al. 2000; NGC 6720, Garnett & Dinerstein 2001; NGC 7009, Krabbe & Copetti 2006), as well as for the HII region 30 Doradus (Tsamis et al. 2003a). The spatial resolution of these however was

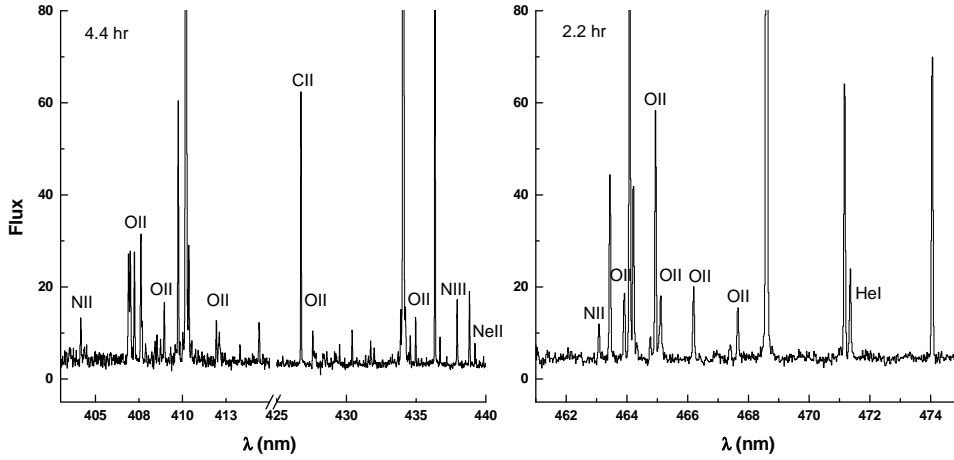


Figure 1. Single $0.52''$ spaxel FLAMES/Argus spectrum of NGC 6153 showing the optical recombination lines from CNONE ions. Note the full complement of O II V1 multiplet ORLs near 4650 \AA .

only moderate (usually worse than $1''/\text{pix}$) and the spectra did not sample the seeing. The FWHM spectral resolution, $\lambda/\Delta\lambda (= R)$, was also not better than ~ 3000 . Similar studies with échelle spectrographs, such as VLT UVES (e.g. Peimbert et al. 2004), fared better in spectral resolution (~ 8800), but the spatial coverage of those was even more restricted.

The advent of integral-field unit (IFU) spectrographs has opened up new options for PN research (see also Roth, this volume). IFUs provide high spatio-spectral resolution over a large field of view: with the use of arrays of small microlenses/fibres the seeing can be sampled and contiguous fibre coverage prevents flux losses, in contrast to long-slit techniques. Our instrument of choice, VLT FLAMES in Argus mode, provides coverage of a $12'' \times 7''$ or $6.6'' \times 4.2''$ field of view at spatial resolutions of $0.52''$ or $0.30''$, respectively, and at medium to high R . In this work we have used FLAMES/Argus to observe the Galactic disk PNe NGC 5882, 7009, and 6153. Our published long-slit studies show that these PNe have ADFs of $\sim 2, 5$ and 10 , respectively. It was argued for a variety of reasons, but primarily since the *ISO* fine-structure CELs yield consistent abundances with the optical CELs, that small-scale temperature fluctuations do not contribute significantly to the observed ORL/CEL abundance discrepancies, and the CEL abundances do provide a representative measure of the gas metallicity in these targets. The CNONE ORL emission, on the other hand, is best explained by the presence of a small amount of gas (1–2% of the total ionized nebular matter) which is hydrogen-deficient, and therefore cold ($\lesssim 1000 \text{ K}$), and which does not emit high-excitation energy UV/optical CELs. Our Argus data allow us to map the two-dimensional distribution of heavy-element ORL vs. CEL emission across the PNe in unprecedented detail and are expected to yield new insights into the astrophysics of these objects.

2. FLAMES/Argus observations

The spectra were obtained in queue mode between March–August 2005 in subarcsec seeing. NGC 7009 was observed with both small and large IFUs, while NGC 5882 & NGC 6153 were observed with the large IFU only. The large IFU covered roughly one quadrant of the surface of NGC 6153 & NGC 7009, and was placed along the radial

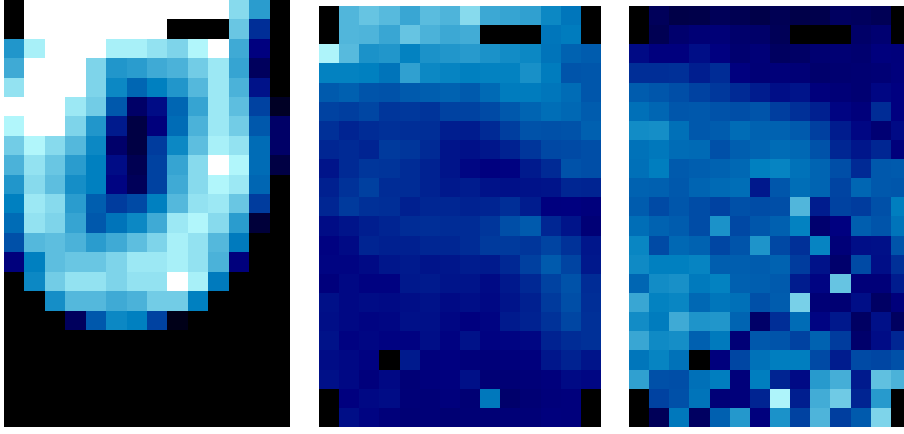


Figure 2. (left): NGC 5882 – [O III] $\lambda 4959$ map (log-scale); (centre): NGC 6153 – forbidden-line O^{2+}/H^+ abundance ratio map; (right): NGC 6153 – ORL O^{2+}/H^+ abundance ratio map. All are $12'' \times 7''$ fields. The blank corner pixels correspond to sky-fibres; those in the 2nd row are dead fibres. See text for details and online version for colour.

direction so as to sample both inner and outer nebular regions. The bright inner shell of NGC 5882 was almost wholly covered with the $12'' \times 7''$ IFU (Fig. 2). Spectra of NGC 7009 (4188–4392, 4538–4759 Å) secured with the small IFU have a R of 32,500 ($=9.2$ km/s) allowing us to measure gas radial velocities to an accuracy of a few km/s: we can thus probe whether heavy element ORLs arise from kinematically distinct regions than CELs in this nebula, by tracking subtle differences in the velocity profiles of CELs vs. ORLs as a function of position on the emission-line maps, and via the detection of asymmetrical profiles/faint line wings (Fig. 3). The 3964–5078 Å spectra of all 3 PNe taken with the large IFU have a R of $\sim 10,000$ – $12,000$ ($=25$ – 30 km/s), comparable to the typical expansion velocity of a PN and thus optimal for the detection of faint ORLs. Fig. 1 shows a representative deep spectrum of NGC 6153 extracted from a *single* $0.52''$ spaxel, reaching weak O II ORLs (of intensity less than 1% that of $H\beta$) at a S/N ratio greater than 10.

3. First results

The data were reduced with the girBLDRS pipeline provided by the Geneva Observatory and flux calibrated within IRAF. Custom-made IRAF routines allowed us to create data cubes and to extract high S/N ratio emission-line maps by fitting Gaussians to the lines. The maps were then dereddened and converted to physical quantities, such as electron temperatures (T_e), densities (N_e) and abundances. In Fig. 2(*left*) the [O III] $\lambda 4959$ map of NGC 5882 is shown. In Fig. 2(*centre*) the forbidden-line O^{2+}/H^+ abundance map of the SE quadrant of NGC 6153 is shown: it was created using an [O III] $\lambda 4959/H\beta$ ratio map, an [O III] $\lambda 4363/\lambda 4959$ T_e map and an [Ar IV] $\lambda 4711/\lambda 4740$ N_e map. The central star is at the bottom-right corner. The mean O^{2+}/H^+ abundance ratio from the map is 3.9×10^{-4} , which compares well with the value of 4.3×10^{-4} from the scanning long-slit ESO 1.52-m study of the entire PN ($27'' \times 34''$) by Liu et al. (2000). In Fig. 2(*right*) the recombination-line O^{2+}/H^+ abundance map of the same region is shown: it was created from an O II $\lambda 4649/H\beta$ ratio map. The mean O^{2+}/H^+ value from that map is 4.0×10^{-3} compared to 2.8×10^{-3} from the scanning long-slit study. The derived ADF for O^{2+} from the ratio of the two NGC 6153 maps ranges from ~ 5 to 20 with decreasing nebular radius and peaks around the central star; this directly implicates the central star itself, or the

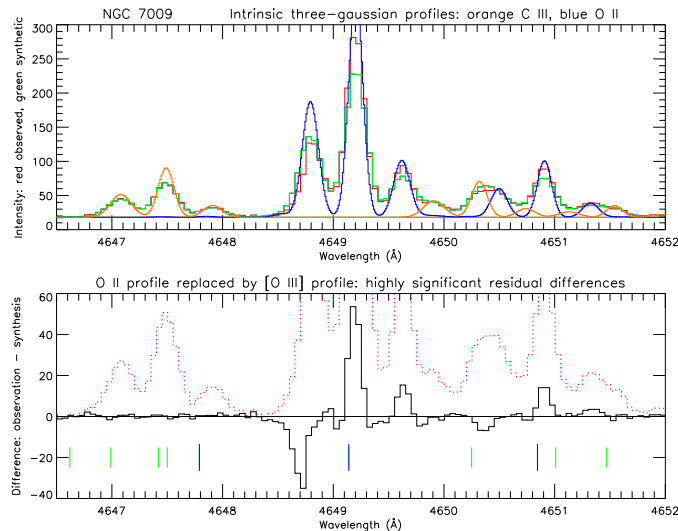


Figure 3. NGC 7009: observed and synthetic spectrum of a $0.9'' \times 0.9''$ region at $R = 32,500$ extracted from the $6.6'' \times 4.2''$ IFU. See text for details and online version for colour.

hard radiation field close to it, in the ORL/CEL discrepancy problem. Maps such as these will also allow us to track the pixel to pixel variation of crucial quantities such as, for example, the T_e from the O II $\lambda 4089/\lambda 4649$ ORL ratio, or the N_e from the intramultiplet intensity ratios of O II V1 ORLs and can throw new light on the nature of the hydrogen-poor nebular component.

Fig. 3 shows the high resolution spectrum of a $0.9'' \times 0.9''$ region in NGC 7009, near the projected edge of the bright inner nebular shell, covering the C III 4647.42, 4650.25, 4651.47 Å and O II 4649.13, 4650.84 Å ORLs. Each line exhibits 3 components with central wavelengths at $\sim -93, -60$ and -28 km/s, probably corresponding to the edge of the inner PN shell (central peak) and the expanding fainter, outer shell (peaks on either side). In the upper panel observed (red) and synthetic (green) spectra are shown. The intrinsic synthetic spectra (before convolution with the instrumental profile) of C III (orange) and O II (blue) are overplotted. The synthetic O II line profiles have been replaced by the profile of [O III] $\lambda 4363$. The bottom panel, which shows the difference between the observed and synthetic spectra, yields large residuals, especially for the central O II peak, i.e. the O II ORLs have significantly narrower widths than [O III] $\lambda 4363$. This indicates that, even though they are emitted from the same O^{2+} ion, the O II ORLs and [O III] $\lambda 4363$ cannot originate from material of identical physical properties.

References

- Garnett, D.R. & Dinerstein, H.L. 2001, *ApJ* 558, 145
 Krabbe, A.C. & Copetti, M. V. F. 2006, *A&A* 450, 159
 Liu, X.-W., Storey, P.J., Barlow, M.J., Danziger, I.J., et al. 2000, *MNRAS* 312, 585
 Liu, Y., Liu, X.-W., Barlow, M.J., Luo, S.-G. 2004, *MNRAS* 353, 1251
 Peimbert, M., Peimbert, A., Ruiz, M.T., Esteban, C. 2004, *ApJS* 150, 431
 Tsamis, Y.G., Barlow, M.J., Liu, X.-W., Danziger, I.J., Storey P.J. 2003a, *MNRAS* 338, 687
 Tsamis, Y.G., Barlow, M.J., Liu, X.-W., Danziger, I.J., Storey, P.J. 2003b, *MNRAS* 345, 186
 Tsamis, Y.G., Barlow, M.J., Liu, X.-W., Storey, P.J., Danziger, I.J. 2004, *MNRAS* 353, 953
 Wesson, R., Liu, X.-W., Barlow, M.J. 2005, *MNRAS* 362, 424